Organic LETTERS

Letter

pubs.acs.org/OrgLett

Indoleamine 2,3-Dioxygenase Inhibitors Isolated from the Sponge *Xestospongia vansoesti*: Structure Elucidation, Analogue Synthesis, and Biological Activity

Ryan M. Centko,[†] Anne Steinø,[‡] Federico I. Rosell,[‡] Brian O. Patrick,[§] Nicole de Voogd,[¶] A. Grant Mauk,*[,‡] and Raymond J. Andersen*[,†]

[†]Departments of Chemistry and Earth, Ocean & Atmospheric Sciences, University of British Columbia, 2036 Main Mall, Vancouver V6T 1Z1, British Columbia, Canada

[‡]Department of Biochemistry and Molecular Biology, University of British Columbia, 2350 Health Sciences Mall, Vancouver V6T 1Z3, British Columbia Canada

[§]Department of Chemistry, University of British Columbia, 2036 Main Mall, Vancouver V6T 1Z1, British Columbia Canada

[¶]Netherlands Centre for Biodiversity Naturalis, P.O. Box 9517, 2300 RA Leiden, The Netherlands

Supporting Information

ABSTRACT: Two new IDO inhibitory meroterpenoids, xestolactone A (**1**) and xestosaprol O (**2**), have been isolated from the sponge *Xestospongia vansoesti*. Xestolactone A (**1**) has an unprecedented degraded meroterpenoid carbon skeleton. A short synthesis of the xestosaprol O (**2**) analogues **3** and **4** features the application of a rarely used photochemical coupling reaction. Synthetic analogue **3** is ~40 times more potent than the inspirational natural product **2**.

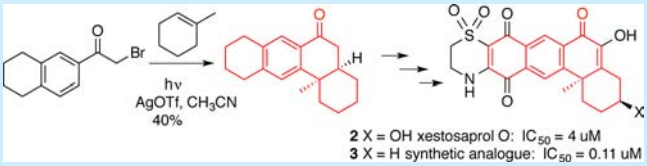

Immune escape plays a central role in the progression of cancer from oncogenesis to metastasis and ultimately a lethal outcome.[1,2] Tumors display immunogenic antigens that would normally be expected to trigger immune rejection, but many tumors ultimately manage to escape destruction by evading or subverting the normal immune response. Recently, there has been much interest in developing noncytotoxic chemotherapeutic agents capable of reversing tumor immune escape mechanisms in order to re-engage the body's immune system in eradicating localized and disseminated tumor cells. Although the mechanisms of tumor immune escape are complex and still not completely understood, the enzyme indoleamine 2,3-dioxygenase (IDO) has emerged as a promising drug target for the reversal of immune escape by tumors.[3−5]

IDO is a monomeric heme enzyme found in nonhepatic human tissues that catalyzes the oxidative cleavage of the 2,3 bond of tryptophan (Trp), the first step in the kynurenine pathway of Trp degradation.[5] This cleavage leads to a local decrease in Trp concentration and generates a variety of catabolic products, which both contribute to the immunosuppressive effects of IDO. T-cells, the immune system component expected to remove antigen presenting tumor cells, must divide to be activated. Trp-deficient microenvironments halt T-cell proliferation by causing cell cycle arrest in G1. Consequently, localized IDO-mediated degradation of Trp at a tumor site is believed to inhibit T-cell activation and proliferation, thereby preventing immunological rejection of the tumor. Several IDO generated catabolites of Trp are reported to be toxic to T-cells, and recently, kynurenine has been identified as a ligand for the aryl hydrocarbon receptor (AhR).[6] It has been suggested that kynurenine-binding to AhR helps tumors generate a pathogenic inflammation in their microenvironment that contributes to immune escape.[5] IDO is constitutively expressed in a large number of human cancers, and IDO expression has been reported to be a marker of poor prognosis.[7]

Data from murine cancer models has provided compelling in vivo evidence for the promise of IDO inhibitors as anticancer drugs.[4,5] A number of structurally diverse natural product and synthetic IDO inhibitors have been reported,[8] including the annulin,[9] exiguamine,[10] and plectosphaeroic acid[11] families of marine natural products. Three IDO inhibitors, D-*N*-methyl-tryptophan (Indoximod), INCB024360, and NLG919, have entered phase I/II clinical trials for evaluation as novel cancer chemotherapeutics designed to reverse tumor escape, but to date there have been no reports of the clinical outcomes from these trials.[5]

A continuation of our screening program aimed at finding structurally novel and potent natural product inhibitors of purified recombinant human IDO[9−11] identified a crude MeOH extract of the marine sponge *Xestospongia vansoesti* collected in the Philippines as a promising hit. Bioassay-guided fractionation of the extract yielded the new natural products xestolactone A (**1**) and xestosaprol O (**2**). Compounds **1** and **2** are related to the well-known family of sponge meroterpenoids

Received: November 17, 2014
Published: December 11, 2014

   dx.doi.org/10.1021/ol503337f | *Org. Lett.* 2014, 16, 6480−6483

that includes helenaquinone,[12] xestoquinone,[13] and the adociaquinones.[14] Members of this family have been reported to be active in phenotypic assays for HIF signaling, cardiotonic, antifungal, cytotoxic, and antimalarial activities and in pure molecular target assays measuring in vitro inhibition of kinase, ATPase, topoisomerase, and phosphatase activities.[15] Xestolactone A (**1**) has an unprecedented degraded meroterpenoid carbon skeleton. Xestosaprol O (**2**) (IC_{50} 4 μM) showed significant in vitro IDO inhibition in contrast with xestolactone A (**1**) (IC_{50} 81 μM) that was only marginally active.

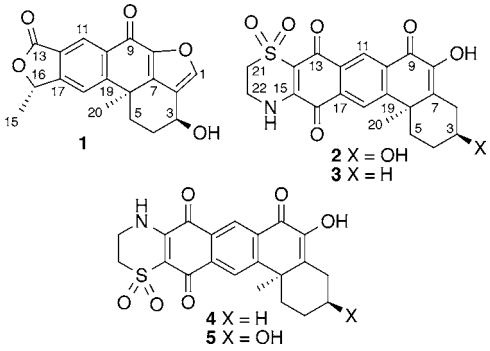

A short synthesis of the xestosaprol O analogues **3** and **4** has been developed in order to generate sufficient material for further biological evaluation of the new IDO inhibitory pharmacophore revealed by **2**. Key steps in the syntheses of **3** and **4** are the use of a photochemical reaction developed by Sato et al.[16] to provide efficient access to the tetracyclic core of the xestosaprol O carbon skeleton and the use of hydoxyquinones to control the regiochemistry of hypotaurine addition. Details of the structure elucidation of **1** and **2**, the syntheses of **3** and **4**, and the IDO inhibitory activities of the natural products and synthetic analogues are presented below.

Lyophilized specimens of *X. vansoesti* were extracted repeatedly with MeOH, and the combined MeOH extracts were concentrated *in vacuo* to give a dark red/brown glass that was sequentially partitioned between hexanes and H_2O and then EtOAc and H_2O. Fractionation of the active EtOAc soluble materials first by Sephadex LH20 chromatography (eluent: 20:80, CH_2Cl_2/MeOH) and then by extensive reversed-phase HPLC gave pure samples of the new compounds **1** and **2**.

Xestolactone A (**1**) was isolated as dark red optically active crystals that gave an $[M + H]^+$ ion in the HRESITOFMS at m/z 325.1070 appropriate for the molecular formula $C_{19}H_{16}O_5$ (calcd 325.1076), requiring 12 sites of unsaturation. The LRESIMS recorded in MeOD gave a $[M + D]^+$ ion at m/z 327, revealing the presence of a single exchangeable proton. Analysis of the ^1H, ^{13}C, and gHSQC NMR spectra of **1** (Figure 1B) identified two carbonyl resonances [δ 169.0, C-13; 169.7, C-9], three aromatic methines [δ 148.7, C-1; 125.8, C-11; 121.1, C-18], and seven quaternary aromatic carbons [δ 127.8, C-2; 147.0, C-7; 144.9, C-8; 135.8, C-10; 126.3, C-12; 156.0, C-17; 158.6, C-19], accounting for seven sites of unsaturation and suggesting that **1** was pentacyclic.

The COSY spectrum of **1** showed a correlation between an oxymethine quartet at δ 5.74 (H-16, J = 7.0 Hz; C-16: δ 79.1) and a methyl doublet at δ 1.71 (H-15, J = 7.0 Hz; C-15: δ 20.9) (Figure 1C). HMBC correlations were observed between the H-16 methine (δ 5.74) and the C-15 methyl carbon resonance at δ 20.9, the carbonyl resonance at δ 169.0 (C-13), the quaternary aromatic resonance at δ 156.0 (C-17), and the

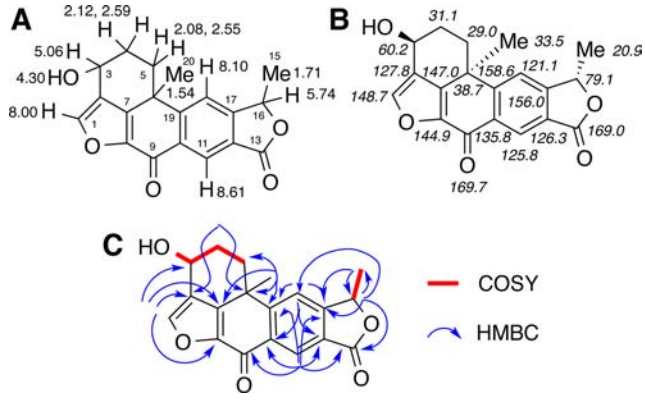

Figure 1. NMR data for xestolactone A (**1**).

aromatic methine resonance at δ 121.1 (C-18) that in turn showed an HSQC correlation to a proton resonance at δ 8.10 (H-18). The H-18 proton resonance (δ 8.10) showed HMBC correlations to four quaternary aromatic resonances at δ 135.8 (C-10), 126.3 (C-12), 156.0 (C-17), and 158.6 (C-19), which all showed additional HMBC correlations to a second aromatic methine resonance at δ 8.61 (H-11), consistent with a 1,2,4,5-tetrasubstituted benzene ring. HMBC correlations between H-18 (δ 8.10) and C-16 (δ 79.1), and between H-16 (δ 5.74) and C-18 (δ 121.1), identified the oxymethine C-16 as one of the four benzene substituents, and an HMBC correlation between H-11 (δ 8.61) and C-13 (δ 169.0), identified the carbonyl as a second substituent. An HMBC correlation between H-16 and C-13, along with the downfield chemical shift of H-16 (δ 5.74) confirmed that C-13 and C-16 were part of a γ lactone fused to the benzene ring as shown in Figure 1. The H-11 resonance at δ 8.61 showed an HMBC correlation to the carbonyl resonance at δ 169.7 (C-9), which situated the carbonyl (C-9) ortho to H-11 as the third substituent on the benzene ring.

COSY and HSQC data routinely identified a three-carbon aliphatic fragment that started with a methylene (C-5), terminated in a carbinol methine (C-3), and accounted for the exchangeable proton identified in the LRESIMS (Figure 1). A methyl resonance at δ 1.54 (H_3-20) showed an HMBC correlation to a quaternary carbon resonance at δ 38.7 (C-6), to the C-5 methylene carbon resonance at δ 29.0, and to the quaternary aromatic carbon resonance at δ 158.6 (C-19), revealing that the quaternary carbon (C-6) bearing the methyl (C-20) was attached to C-5 and was the fourth substituent on the tetrasubstituted benzene ring.

A proton resonance at δ 8.00 (H-1) showed HMBC correlations to quaternary sp^2 carbon resonances at δ 127.8 (C-2), 147.0 (C-7), and 144.9 (C-8) that were assigned to a trisubstituted furan ring. The chemical shift of the proton (δ 8.00) and the carbon it was attached to (δ 148.7, C-1) were consistent with the proton being at the α position of the furan. HMBC correlations between H-1 (δ 8.00) and the carbinol methine resonance at δ 60.2 (C-3), and between the methyl resonance at δ 1.54 (H_3-20) and the furan carbon resonance at δ 147.0 (C-7), identified C-3 and C-6 as the β substituents on the furan as shown in Figure 1. Linking the C-9 carbonyl to the second furan α carbon (C-8) completed the final ring that was needed in **1** to satisfy the unsaturation number required by the molecular formula.

tROESY correlations observed between Me-20 (δ 1.54), H-4a (δ 2.59), and H-5a (δ 2.55) and between H-5a (δ 2.55) and H-3 (δ 5.06) established the *trans* relative configuration

dx.doi.org/10.1021/ol503337f | *Org. Lett.* 2014, 16, 6480−6483

between Me-20 and OH-3 as shown in Figure 1**B**. However, there was no way to establish the relative configuration at C-16 using NOE data. Fortunately, xestolactone A (**1**) crystallized from acetone and single-crystal X-ray diffraction analysis confirmed the constitution established by analysis of NMR data and assigned the absolute configuration as 3*S*,6*R*,16*S* (Figure 2 and Supporting Information).

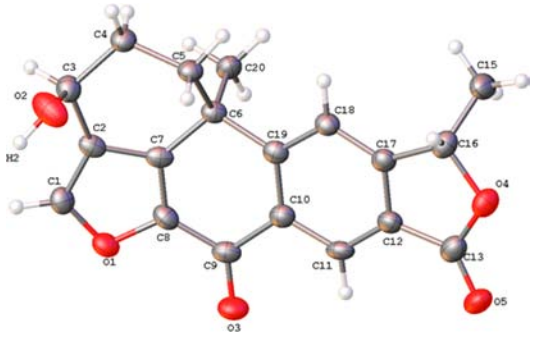

Figure 2. ORTEP diagram generated for xestolactone A (**1**).

Xestosaprol O (**2**) was isolated as an optically active yellow solid that gave a $[M + Na]^+$ ion in the HRESITOFMS at *m*/*z* 452.0774, appropriate for the molecular formula $C_{21}H_{19}NO_7S$ (calcd 452.0780) requiring 14 sites of unsaturation. The molecular formula and the ^1H and ^{13}C NMR spectra obtained for **2** were nearly identical to those reported for xestosaprol N (**5**) (Table 1, Supporting Information).[17] Analysis of the 1D and 2D NMR data for **2** revealed the diosphenol, naphthoquinone, dioxydihydrothiazine ring, and methyl cyclohexyl ring system substructures present in xestosaprol N (**5**). However, careful inspection of the 2D NMR data obtained for **2** revealed that the aromatic methine H-18 (δ 8.33) showed strong HMBC correlations to the most deshielded carbonyl resonance at δ 178.5 (C-16), while the other aromatic methine resonance H-11 (δ 8.63) showed HMBC correlations to the diosphenol carbonyl resonance at δ 177.0 (C-9) and the more shielded quinone carbonyl resonance at δ 173.0 (C-13). This suggested that the orientation of the thiazine ring system present in xestosaprol N (**5**) was reversed in xestosaprol O (**2**). Weak HMBC correlations from the N–H (δ 9.23) to C-15 (δ 146.8) and C-16 (δ 178.5) supported the assigned thiazine regiochemistry in xestosaprol O (**2**), which was confirmed by analysis of the HMBC data obtained for the analogues **3** and **4** prepared by unambiguous synthesis (vide infra and Supporting Information). tROESY data showed that the C-3 OH and Me-20 were *trans* as in **1**. On the basis of the assumption of a common biogenesis for **1** and **2**, the absolute configuration of **2** was assigned as 3*S*,6*R*.

Xestolactone A (**1**) has an unprecedented degraded meroterpenoid carbon skeleton. A proposal for the degradation sequence is shown in the Supporting Information.

The natural product xestosaprol O (**2**) showed in vitro inhibition of IDO that warranted further biological evaluation. However, the limited amounts of this compound available from the sponge source precluded further studies. To solve the supply problem and at the same time explore the SAR of the new IDO inhibitory pharmacophore represented by **2**, we developed a short synthesis of analogues of the natural product.

Total syntheses of helenaquinone,[18] adociaquinone,[19] and xestoquinone[20] that contain the C-1/C-2/C-7/C-8 furan substructure common in this family have been reported, but there are no reports of the synthesis of a C-1 nor diosphenol-containing member of the family. Therefore, we turned our attention to the synthesis of the xestosaprol O (**2**) analogue **3**, which is just missing the 3-hydroxyl substituent.

Our synthetic approach to **3** was designed to take advantage of the photochemical coupling reaction between methylcyclohexene and chloroacetophenone **6** shown in Scheme 1 that was

Scheme 1. Sato Photochemical Coupling Reaction[16]

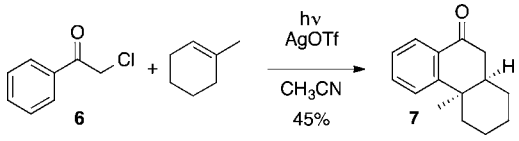

discovered 30 years ago by Sato et al.[16] but has never been exploited in a natural product synthesis. The reaction is reported to proceed in reasonable yield from **6** to the methylphenanthrenone **7** that has a *cis* decalin ring junction and a tricyclic carbon skeleton identical to a core fragment of **3**. We anticipated that extension of the Sato reaction to an appropriately functionalized chloroacetylnaphthalene would efficiently generate the tetracyclic skeleton of **3** in one synthetic step. However, all attempts to carry out the Sato reaction with variously substituted haloacetylnaphthalenes failed to produce the desired coupling products.

Fortunately, the bromoacetyltetrahydronaphthalene **9**[21] reacted with methylcyclohexene under the Sato photochemical conditions to give the tetracyclic coupling product **10** (Scheme 2) with the *cis* decalin ring junction and desired regiochemistry.

Scheme 2. Synthesis of Analogues 3 and 4

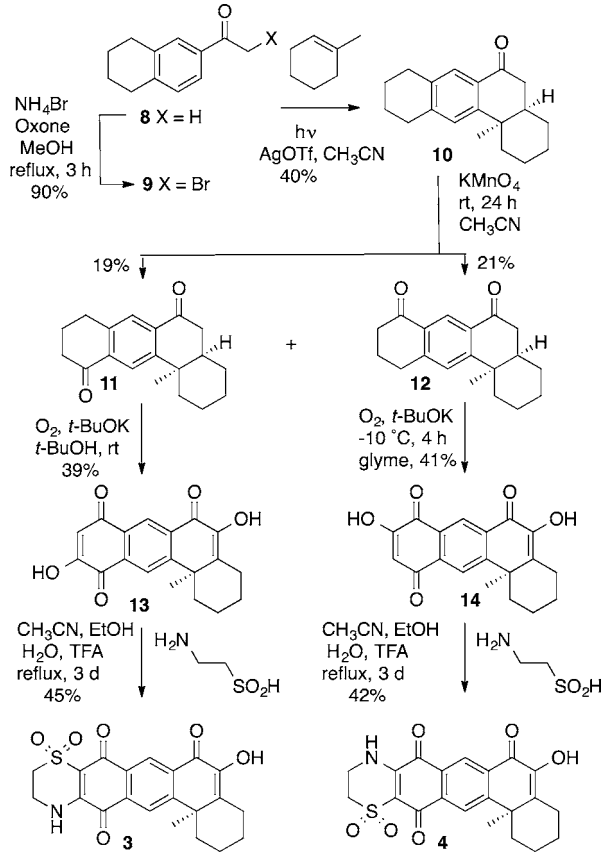

dx.doi.org/10.1021/ol503337f | *Org. Lett.* 2014, 16, 6480–6483

Oxidation of **10** with $KMnO_4$ in acetonitrile gave the mixture of regioisomeric ketones **11** and **12** that could be easily separated by Si gel chromatography. The locations of the ketone functionalities in **11** and **12** were unambiguously assigned on the basis of HMBC correlations observed from the aromatic methine protons (Supporting Information). Further oxidation of **11** with molecular oxygen in the presence of *t*-BuOK installed in one step both the diosphenol[22] and hydroxyquinone[23] functionalities in **13**. Reaction of **13** with hypotaurine for 3 days in a refluxing mixture of CH_3CN, EtOH, H_2O, and TFA gave the desired addition product **3** as a single regioisomer.[24] Exposing the ketone **14** to a similar sequence of oxygenation and hypotaurine addition reactions gave the analogue **4** as a single regioisomer. The use of hydroxyquinones to direct the regiochemistry of hypotaurine addition to a xestoquinone scaffold is a useful new addition to the methodology for making dioxydihydrothiazine containing natural products in this family.

Xestosaprol O (**2**) (IC_{50} 4 μM) represents a promising new IDO inhibitory pharmacophore. The synthetic xestosaprol O (**2**) analogue **3** (IC_{50} 0.11 μM), which differs from the natural product only by the absence of the C-3 hydroxyl substituent, is roughly 40 times more potent than the natural product and has a submicromolar IC_{50}. The increase in potency of **3** compared with **2** reveals that the C-3 hydroxyl is significantly detrimental to the IDO inhibitory potency of this pharmacophore. Comparison of the potencies of the synthetic intermediates **13** (IC_{50} 80 μM), and **14** (IC_{50} 10 μM), with the corresponding hypotaurine adducts **3** (IC_{50} 0.11 μM), and **4** (IC_{50} 1.4 μM), illustrates the importance of the dioxydihydrothiazine rings for IDO inhibition. The regioisomer **4** is roughly an order of magnitude less potent than **3**, revealing that the orientation of the dioxydihydrothiazine ring fusion to C-14/C-15 is also crucial.

In summary, the new IDO inhibitory meroterpenoids **1** and **2** have been isolated from the sponge *X. vansoeti*. One of them, xestolactone A (**1**), has an unprecedented meroterpenoid carbon skeleton, and a second one, xestosaprol O (**2**), has served as a lead compound for the development of a significantly more potent synthetic analogue **3**. The synthesis of **3** features the first application of a photochemical coupling reaction discovered by Sato to the construction of a natural product scaffold. Use of the Sato coupling reaction combined with two highly effective oxidative steps furnished a short and regioselective synthetic approach to **3**, which is capable of providing material for further in vitro and in vivo evaluation of this new meroterpenoid IDO inhibitory pharmacophore.

■ ASSOCIATED CONTENT

Supporting Information

NMR data for compounds **1**−**14**, X-ray data for **1**, and experimental procedures. This material is available free of charge via the Internet at http://pubs.acs.org.

■ AUTHOR INFORMATION

Corresponding Authors

* E-mail: grant.mauk@ubc.ca.
* E-mail: raymond.andersen@ubc.ca.

Notes

The authors declare no competing financial interest.

■ ACKNOWLEDGMENTS

Financial support was provided by grants to R.J.A. and A.G.M. from the Canadian Cancer Society.

■ REFERENCES

(1) Prendergast, G. C.; Metz, R.; Muller, A. J. *Am. J. Pathol.* **2010**, *176*, 2082−2087.
(2) Smith, C.; Chang, M. Y.; Parker, K. H.; Beury, D. W.; DuHadaway, J. B.; Flick, H. E.; Boulden, J.; Sutanto-Ward, E.; Soler, A. P.; Laury-Kleintop, L. D.; Mandik-Nayak, L.; Metz, R.; Ostrand-Rosenberg, S.; Prendergast, G. C.; Muller, A. J. *Cancer Discovery* **2012**, *2*, 722−735.
(3) Johnson, T. S.; Munn, D. H. *Immunol. Invest.* **2012**, *41*, 765−797.
(4) Liu, X.; Shin, N.; Koblish, H. K.; Yang, G.; Wang, Q.; Wang, K.; Leffet, L.; Hansbury, M. J.; Thomas, B.; Rupar, M.; Waeltz, P.; Bowman, K. J.; Polam, P.; Sparks, R. B.; Yue, E. W.; Li, Y.; Wynn, R.; Fridman, J. S.; Burn, T. C.; Combs, A. P.; Newton, R. C.; Scherle, P. A. *Blood* **2010**, *115*, 3520−3530.
(5) Prendergast, G. C.; Smith, C.; Thomas, S.; Mandik-Nayak, L.; Laury-Kleintop, L.; Metz, R.; Muller, A. J. *Cancer Immunol. Immunother.* **2014**, *63*, 721−735.
(6) Platten, M.; Wick, W.; Van den Eynde, B. J. *Cancer Res.* **2012**, *72*, 5435−5440.
(7) Folgiero, V.; Goffredo, B. M.; Filippini, P.; Masetti, R.; Bonanno, G.; Caruso, R.; Bertaina, V.; Mastronuzzi, A.; Gaspari, S.; Zecca, M.; Torelli, G. F.; Testi, A. M.; Pession, A.; Locatelli, F.; Rutella, S. *Oncotarget* **2014**, *5*, 2052−2064.
(8) Dolusic, E.; Frederick, R. *Expert Opin. Ther. Patents* **2013**, *23*, 1367−1381.
(9) Pereira, S. A.; Vottero, E.; Roberge, M.; Mauk, A. G.; Andersen, R. J. *J. Nat. Prod.* **2006**, *69*, 1496−1499.
(10) Brastianos, H.; Vottero, E.; Patrick, B. O.; Van Soest, R.; Matainaho, T.; Mauk, A. G.; Andersen, R. J. *J. Am. Chem. Soc.* **2006**, *128*, 16046−16047.
(11) Carr, G.; Tay, W.; Bottriell, H.; Andersen, S. K.; Mauk, A. G.; Andersen, R. J. *Org. Lett.* **2009**, *11*, 2996−2999.
(12) Roll, D. M.; Scheuer, P. J.; Matsumoto, G. K.; Clardy, J. *J. Am. Chem. Soc.* **1983**, *105*, 6177−6178.
(13) Nakamura, H.; Kobayashi, J.; Kobayashi, M.; Ohizumi, Y.; Hirata, T. *Chem. Lett.* **1985**, 713−716.
(14) Schmitz, F. J.; Bloor, S. J. *J. Org. Chem.* **1988**, *53*, 3922−3925.
(15) Du, L.; Mahdi, F.; Datta, S.; Jekabsons, M. B.; Zhou, Y.-D.; Nagle, D. G. *J. Nat. Prod.* **2012**, *75*, 1553−1559 and references therein.
(16) Sato, T.; Tamura, K. *Tetrahedron Lett.* **1984**, *25*, 1821−1824.
(17) Lee, Y.-J.; Kim, C.-K.; Park, S.-K.; Kang, J. S.; Lee, J. S.; Shin, H. J.; Lee, H.-S. *Heterocycles* **2012**, *85*, 895−901.
(18) Kienzler, M. A.; Suseno, S.; Trauner, D. *J. Am. Chem. Soc.* **2008**, *130*, 8604−8605.
(19) Harada, N.; Sugioka, T.; Soutome, T.; Hiyoshi, N.; Uda, H.; Kuriki, T. *Tetrahedron Asymmetry* **1995**, *6*, 375−376.
(20) Sutherland, H. S.; Higgs, K. C.; Taylor, N. J.; Rodrigo, R. *Tetrahedron* **2001**, *57*, 309−317.
(21) Macharla, A. K.; Nappunni, R. C.; Marri, M. R.; Perka, S.; Nama, N. *Tetrahedron Lett.* **2012**, *53*, 191−195.
(22) Harada, N.; Sugioka, T.; Uda, H.; Kuriki, T.; Kobayashi, M.; Kitagawa, I. *J. Org. Chem.* **1994**, *59*, 6606−6613.
(23) Malerich, J. P.; Maimone, T. J.; Elliott, G. I.; Trauner, D. *J. Am. Chem. Soc.* **2005**, *127*, 6276−6283.
(24) Bala, B. D.; Muthusaravanan, S.; Perumal, S. *Tetrahedron Lett.* **2013**, *54*, 3735−3739.